

$[(C_5Me_5)Rh(Nb_2W_4O_{19})]^{2-2}$ and $[(C_5Me_5)Rh]_4(Mo_4O_{16})^8$. The $V_6O_{19}^{8-}$ core has the same structure as the $Nb_6O_{19}^{8-}$, $Ta_6O_{19}^{8-}$, $Mo_6O_{19}^{2-}$, and $W_6O_{19}^{2-}$ ions.^{1c} It thus represents the first observation of this hexametallate structure in polyvanadate chemistry, although mixed-metal species incorporating vanadium are known.^{1c}

Preliminary experiments indicate that several organo-transition-metal hydroxides are reactive toward both main-group and transition-metal oxides, demonstrating that the synthetic approach described here has considerable generality, particularly when hydrothermal techniques are employed.

Acknowledgment. We acknowledge the National Science Foundation for partial support of this work. H.K.C. was supported by the U.S. Department of Energy, Division of Materials Science, under Contract DE-AC02-76ER01198. We are grateful to Dr. Atsushi Yagasaki for bringing ref 5 to our attention.

- (9) The first number in parentheses following an averaged value of a bond length or angle is the root-mean-square estimated standard deviation of an individual datum. The second and third numbers are the average and maximum deviations from the averaged value, respectively. The fourth number represents the number of individual measurements included in the averaged value.
- (10) Cg refers to the center of gravity for the five-membered ring of a $(CH_3)_5C_5^-$ ligand.

Supplementary Material Available: Crystal structure analysis report, Table I (fractional atomic coordinates for non-hydrogen atoms), Table II (anisotropic thermal parameters for non-hydrogen atoms), Table III (atomic coordinates for hydrogen atoms), Table IV [bond lengths and angles in $[(C_5Me_5)Rh]_4(V_6O_{19})$], Table V (bond lengths and angles in solvent molecules), Figure 2 [perspective thermal vibration ellipsoid drawings of $[(C_5Me_5)Rh]_4(V_6O_{19})$], Figure 3 [perspective drawing of $[(C_5Me_5)Rh]_4(V_6O_{19})$ including locatable hydrogen atoms], and Figure 4 (perspective drawings of solvent molecules in 1) (18 pages); structure factor tables for the crystal structure analysis of 1 (10 pages). Ordering information is given on any current masthead page.

Department of Chemistry and Materials
Research Laboratory
University of Illinois
Urbana, Illinois 61801

H. K. Chae
W. G. Klemperer*

Crystallitics Company
Lincoln, Nebraska 68501
Department of Chemistry
University of Nebraska
Lincoln, Nebraska 68588

V. W. Day*

Received November 8, 1988

Articles

Contribution from the Department of Chemistry,
Rice University, Houston, Texas 77251

Synthesis and Characterization of a Series of Antimony-Containing Iron Carbonyl Complexes: $[Et_4N]_3[SbFe_4(CO)_{16}]$, $[Et_4N]_2[HSbFe_4(CO)_{13}]$, $[Et_4N][H_2SbFe_4(CO)_{13}]$, and $[Et_4N]_2[CISbFe_3(CO)_{12}]$

Shifang Luo and Kenton H. Whitmire*

Received August 8, 1988

Reactions of $SbCl_3$ or $SbCl_5$ with $Na_2[Fe(CO)_4] \cdot 3/2$ dioxane or with $Fe(CO)_5/KOH/MeOH$ yield the anion $[SbFe_4(CO)_{16}]^{3-}$, which can be easily isolated as its $[Et_4N]^+$ salt, $[Et_4N]_3[I]$, which crystallizes in the monoclinic centrosymmetric space group $P2_1/n$ with $a = 13.415$ (2) Å, $b = 19.601$ (2) Å, $c = 19.156$ (2) Å, $\beta = 90.973$ (9)°, $Z = 4$, and $V = 5036.3$ (9) Å³. The Sb atom in this anion is tetrahedrally surrounded by four $Fe(CO)_4$ units with an average Sb-Fe bond distance of 2.666 (3) Å. When treated with 1 equiv of trifluoromethanesulfonic acid (CF_3SO_3H), $[Et_4N]_3[I]$ is converted into $[Et_4N]_2[HSbFe_4(CO)_{13}]$ ($[Et_4N]_2[II]$), in which the Sb atom caps a closed Fe_3 triangle and donates its lone pair of electrons to an external $Fe(CO)_4$ unit. $[Et_4N]_2[Sb_2Fe_3(CO)_{17}]$ is observed as a minor product of this reaction. $[Et_4N]_2[II]$ crystallizes in the monoclinic centrosymmetric space group $P2_1/c$ with $a = 13.805$ (6) Å, $b = 18.934$ (9) Å, $c = 15.295$ (6) Å, $\beta = 97.76$ (6)°, $Z = 4$, and $V = 3961$ (3) Å³. The ¹H NMR spectrum shows a singlet at $\delta = -19.74$ ppm for the hydride ligand. When $[Et_4N]_2[II]$ is treated with an additional 1 equiv of trifluoromethanesulfonic acid, $[Et_4N][H_2SbFe_4(CO)_{13}]$ ($[Et_4N][III]$) is formed. $[Et_4N][III]$ crystallizes in the triclinic centrosymmetric space group $P\bar{1}$ with $a = 12.714$ (2) Å, $b = 14.342$ (2) Å, $c = 8.970$ (2) Å, $\alpha = 99.57$ (1)°, $\beta = 105.27$ (1)°, $\gamma = 82.34$ (1)°, $Z = 2$, and $V = 1549.0$ (4) Å³. The ¹H NMR spectrum shows a singlet at $\delta = -22.63$ ppm for the hydride ligands. The cluster structure is virtually identical with that of $[II]^{2-}$ with an extra bridging H ligand. When treated with 1 equiv of $TiCl_3$ or $SbCl_5$, $[Et_4N]_3[I]$ produces $[Et_4N]_2[CISbFe_3(CO)_{12}]$ ($[Et_4N]_2[IV]$), in which Sb is tetrahedrally bound to one Cl^- and three $Fe(CO)_4$ units, as determined by X-ray diffraction at -80 °C: $[Et_4N]_2[IV] \cdot 0.5CH_2Cl_2$, monoclinic centrosymmetric space group $C2/c$ with $a = 29.30$ (1) Å, $b = 18.500$ (6) Å, $c = 16.844$ (6) Å, $\beta = 119.58$ (2)°, $Z = 8$, and $V = 7942$ (6) Å³.

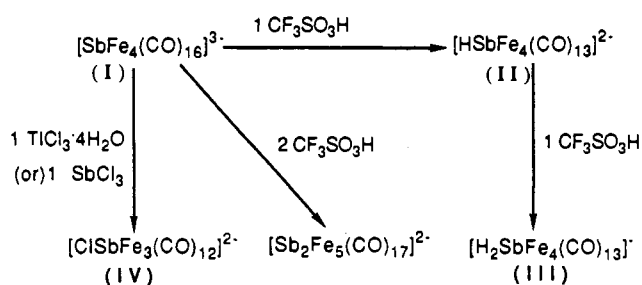
Introduction

Recent studies involving the incorporation of heavy main-group elements into transition-metal clusters have led to a number of exciting molecules with unexpected structure and bonding patterns.^{1,2} Notable examples are $[(\mu_3, \eta^2-E_2)\{W(CO)_5\}_3]$ [$E = As, Sb, Bi$] with very short E-E distances and electron deficient EM_3 molecules like $[CpMn(CO)_2]_3As$,⁶ $[Cr(CO)_5]_2[Mn(CO)_5]As$,⁷

$[Cr_2(CO)_9][Mn(CO)_5]As$,⁷ $[Mn(\eta^5-C_5H_4Me)(CO)_2]_3Te$,⁸ and $[Et_4N]_2[EF_3(CO)_{12}]^{2-}$ ($E = Pb, Sn$).⁹ In $[(\eta^5-C_5H_5)Mo]_2-[\mu, \eta^4-As_5]$ ¹⁰ a planar As_5 ring is capped on opposite sides by two $[\eta^5-CpMo]$ fragments. The structure of $[Et_4N]_2[Bi_4Fe_4(CO)_{13}]^{11}$

- (1) Herrmann, W. A. *Angew. Chem., Int. Ed. Engl.* **1986**, *25*, 57-76.
 (2) Whitmire, K. H. *J. Coord. Chem.* **1988**, *17*, 95-204.
 (3) Sigwarth, B.; Zsolnai, L.; Berke, H.; Huttner, G. *J. Organomet. Chem.* **1982**, *226*, C5.
 (4) Huttner, G.; Weber, U.; Sigwarth, B.; Scheidsteger, O. *Angew. Chem., Int. Ed. Engl.* **1982**, *21*, 215.
 (5) Huttner, G.; Weber, U.; Zsolnai, L. *Z. Naturforsch.* **1982**, *B37*, 707.

- (6) Herrmann, W. A.; Koumbouris, B.; Schafer, A.; Zahn, T.; Ziegler, M. L. *Chem. Ber.* **1985**, *118*, 2472.
 (7) Huttner, G.; Weber, U.; Sigwarth, B.; Scheidsteger, O.; Lang, H.; Zsolnai, L. *J. Organomet. Chem.* **1985**, *282*, 331.
 (8) Herrmann, W. A.; Rohrmann, J.; Ziegler, M. L.; Zahn, T. *J. Organomet. Chem.* **1984**, *273*, 221.
 (9) Cassidy, J. M.; Whitmire, K. H. *Inorg. Chem.*, in press.
 (10) Dehnicke, K.; Strahle, J. *Angew. Chem., Int. Ed. Engl.* **1981**, *20*, 413.
 (11) Whitmire, K. H.; Albright, T. A.; Kang, S.-K.; Churchill, M. R.; Fettingner, J. C. *Inorg. Chem.* **1986**, *25*, 2799.

Scheme I. Reactions of $[\text{SbFe}_4(\text{CO})_{16}]^{3-}$ 

is related to that of the Zintl ions.¹²

Previous work on the heaviest main-group-15 element, Bi, has produced a number of classically bonded Bi-containing clusters showing a variety of bonding patterns. Both open and closed examples are known for three-coordinate complexes: $\text{BiCo}_3(\text{CO})_{12}$,¹³ $\text{BiMn}_3(\text{CO})_{15}$,¹⁴ $\text{Bi}[\text{CpFe}(\text{CO})_2]_3$,¹⁵ $\text{BiCo}_3(\text{CO})_9$,¹⁶ $\text{Bi}_2\text{Fe}_3(\text{CO})_9$,¹⁷ $\text{Bi}_2\text{Os}_3(\text{CO})_9$,¹⁸ $\text{Bi}_2\text{Ru}_3(\text{CO})_9$,¹⁸ and $[\text{Et}_4\text{N}][\text{BiFe}_3(\text{CO})_{10}]$.¹⁹ Four-coordinate Bi is known in $[\text{Cp}_2\text{Co}][\text{BiCo}_4(\text{CO})_{10}]$,²⁰ $[\text{Et}_4\text{N}][\text{BiFe}_4(\text{CO})_{16}]$,²¹ $[\text{Et}_4\text{N}]_2[\text{Bi}_2\text{Fe}_4(\text{CO})_{13}]$,²² $\text{Bi}_2\text{Os}_4(\text{CO})_{12}$,¹⁸ and $\text{Bi}_2\text{Ru}_4(\text{CO})_{12}$.¹⁸ More complex bonding modes of Bi are found in $[\text{Et}_4\text{N}][\text{Bi}_2\text{Fe}_2\text{Co}(\text{CO})_{10}]$ ²² and $[\text{Cp}_2\text{Co}][\text{Bi}_2\text{Co}_4(\text{CO})_{11}]$.²³ Transformations of Bi-Fe clusters reveal Bi greatly influences reactivity and structure by steric and electronic factors.²⁴

On the other hand, fewer complexes containing Sb—the next heaviest main-group-15 element—have been reported, but the number is increasing. Among those known are $[\text{Et}_4\text{N}]_3\text{-}[\text{Rh}_{12}\text{Sb}(\text{CO})_{27}]$,²⁵ $[\text{Et}_4\text{N}][\text{SbFe}_4(\text{CO})_{14}]$,²⁶ $[\text{Et}_4\text{N}]_2[\text{Sb}_2\text{Fe}_5(\text{CO})_{17}]$,²⁶ $\text{Sb}_2\text{Fe}_6(\text{CO})_{22}$,²⁷ $\text{Sb}_2\text{W}_3(\text{CO})_{15}$,³ and $\text{Ph}_2\text{Sb}_2\text{W}_3(\text{CO})_{15}$.³ The distibene π complex $(\text{Me}_3\text{Si})_2\text{CHSb}_2[\text{Fe}(\text{CO})_4]^{28}$ and the stibinidene cluster $(\text{Me}_3\text{Si})\text{CHSb}[\text{Fe}_2(\text{CO})_8]^{28}$ have also been reported.

We were interested in developing methods leading to transition-metal-main-group clusters that might have a structural relationship to Zintl ions and have thus pursued the synthesis of Sb-containing transition-metal complexes. The synthetic approaches employed for Bi are not always successful for antimony. Thus, NaBiO_3 , a powerful oxidizing reagent, is an excellent source of Bi. It quickly reacts with $\text{Fe}(\text{CO})_5$ or $\text{Fe}(\text{CO})_5/\text{KOH}/\text{MeOH}$, yielding $[\text{Et}_4\text{N}][\text{BiFe}_3(\text{CO})_{10}]$ ¹⁹ or $[\text{Et}_4\text{N}]_3[\text{BiFe}_4(\text{CO})_{16}]$ ²¹ in high yield. NaSbO_3 , on the other hand, reacts only slowly with $\text{Fe}(\text{CO})_5$ under reflux. The product of this reaction is $[\text{Et}_4\text{N}]_2\text{-}$

$[\text{Sb}_2\text{Fe}_5(\text{CO})_{17}]$ in low yield.²⁶ With $\text{Fe}(\text{CO})_5/\text{KOH}/\text{MeOH}$, no reaction occurs. While those attempts were not satisfying, a number of new antimony-containing compounds have been synthesized and structurally characterized beginning with antimony chlorides as starting materials. In this paper, we report the synthesis and structural characterization of four Sb-containing iron carbonyl compounds— $[\text{Et}_4\text{N}]_3[\text{SbFe}_4(\text{CO})_{16}]$ ($[\text{Et}_4\text{N}]_3[\text{I}]$), $[\text{Et}_4\text{N}]_2[\text{HSbFe}_4(\text{CO})_{13}]$ ($[\text{Et}_4\text{N}]_2[\text{II}]$), $[\text{Et}_4\text{N}][\text{H}_2\text{SbFe}_4(\text{CO})_{13}]$ ($[\text{Et}_4\text{N}][\text{III}]$), and $[\text{Et}_4\text{N}]_2[\text{ClSbFe}_3(\text{CO})_{12}]$ ($[\text{Et}_4\text{N}]_2[\text{IV}]$)—and their interconversions (see Scheme I). Comparisons to Bi-containing compounds are also made.

Experimental Section

All manipulations were carried out under an atmosphere of dry N_2 by using standard Schlenk techniques. Reagents were used without purification except SbCl_5 , which was sublimed before use. Organic solvents were distilled from standard drying agents and purged with prepurified dry N_2 for 20 min. Infrared spectra were taken on a PE 1430 spectrophotometer, and ^1H NMR were measured on an IBM AF-300 NMR spectrometer. Elemental analyses were obtained from Galbraith Laboratories, Inc.

Synthesis of $[\text{Et}_4\text{N}]_3[\text{I}]$. Method 1. Reaction of SbCl_5 with $\text{Na}_2[\text{Fe}(\text{CO})_4]^{3-}/_2$ diox (diox = Dioxane). SbCl_5 (0.50 g, 2.21 mmol) and $\text{Na}_2[\text{Fe}(\text{CO})_4]^{3-}/_2$ diox (2.68 g, 7.74 mmol) were dissolved in MeCN. The solution turned reddish brown immediately. After the solution was stirred for 12 h, it was filtered and the solvent removed from the filtrate under vacuum. The solid residue was dissolved in MeOH and a solution of 2.0 g of $[\text{Et}_4\text{N}]\text{Br}$ in 30 mL of MeOH added. A red precipitate was collected by filtration, washed with MeOH, and dried under vacuum. Yield: 1.19 g, 45% based on Sb.

Method 2. Reaction of SbCl_5 with $\text{Fe}(\text{CO})_5/\text{KOH}/\text{MeOH}$. $\text{Fe}(\text{CO})_5$ (0.26 mL, 1.9 mmol) was added to a solution of 0.30 g of KOH in 15 mL of MeOH that had been purged with N_2 . A degassed solution of SbCl_5 (0.10 g, 0.45 mmol) in 15 mL of MeOH was added, upon which the solution turned red immediately. The solution was refluxed overnight, cooled, and then filtered. A 2.01-g amount of $[\text{Et}_4\text{N}]\text{Br}$ in 20 mL of MeOH was added to the filtrate, giving a red precipitate that was collected as before. Yield: 0.21 g, 40% based on Sb.

Method 3. Reaction of SbCl_5 with $\text{Na}_2[\text{Fe}(\text{CO})_4]^{3-}/_2$ diox. $\text{Na}_2[\text{Fe}(\text{CO})_4]^{3-}/_2$ diox (10.8 g, 31.3 mmol) was dissolved in 100 mL of MeCN. SbCl_5 (1.0 mL, 7.8 mmol) was added to the solution, which turned reddish brown immediately. After being stirred for 24 h, the solution was filtered and the MeCN removed under vacuum. The solid residue was dissolved in MeOH and an excess amount of $[\text{Et}_4\text{N}]\text{Br}$ in MeOH added. A red precipitate developed and was collected as before. Yield: 5.05 g, 55% based on Sb.

Method 4. Reaction of SbCl_5 with $\text{Fe}(\text{CO})_5/\text{KOH}/\text{MeOH}$. To a solution of 4.4 g of KOH in 30 mL of MeOH was added 4.4 mL of $\text{Fe}(\text{CO})_5$ (33 mmol) and then 1.0 mL of SbCl_5 (7.8 mmol). The solution turned reddish brown immediately upon addition of SbCl_5 . This solution was refluxed overnight, cooled, and filtered. An 8.0-g amount of $[\text{Et}_4\text{N}]\text{Br}$ in 20 mL of MeOH solution was added to the filtrate. The red precipitate was collected as before. Yield: 3.73 g, 41% based on Sb.

Purification of $[\text{Et}_4\text{N}]_3[\text{I}]$ was carried out by dissolving the compound in a minimum volume of MeCN followed by precipitation with MeOH or CH_2Cl_2 . It is soluble in MeCN and THF but insoluble in most other organic solvents. IR (MeCN, cm^{-1}): 1971 s, 1910 m, 1882 m. Visible spectrum (MeCN): 480 nm, $\epsilon \sim 2800$. Anal. Calcd: Sb, 10.28; Fe, 18.87. Found: Sb, 9.67; Fe, 18.39. The crystal for X-ray diffraction was grown by slow diffusion of hexane into a 1:1 MeCN/ CH_2Cl_2 solution.

Synthesis of $[\text{Et}_4\text{N}]_2[\text{II}]$. Method 1. Reaction of $\text{SbCl}_5/\text{MeOH}$ with $\text{Fe}(\text{CO})_5/\text{KOH}/\text{MeOH}$. SbCl_5 (1.0 mL, 7.8 mmol) was added to 20 mL of MeOH. This solution was purged with N_2 for 10 min, and then a solution of 4.4 mL of $\text{Fe}(\text{CO})_5$ (33 mmol) and 4.4 g of KOH in 20 mL of MeOH was added. The solution turned brown within 10 min. It was then refluxed for 30 h and filtered, and the filtrate was treated with 8.0 g of $[\text{Et}_4\text{N}]\text{Br}$ dissolved in methanol. The brown precipitate was collected by filtration and dried under vacuum. Yield: 5.8 g, 76% based on Sb.

Method 2. Reaction of $[\text{Et}_4\text{N}]_3[\text{I}]$ with $\text{CF}_3\text{SO}_3\text{H}$. $[\text{Et}_4\text{N}]_3[\text{I}]$ (0.669 g, 0.565 mmol) was placed in a Schlenk flask and dissolved in MeCN, and then trifluoromethanesulfonic acid (0.05 mL, 0.6 mmol) was added to the red solution, causing it to turn brown immediately. The solution was refluxed for 6 h and filtered, and the solvent MeCN was removed under vacuum. The solid residue was dissolved in MeOH and filtered. Crystals were obtained upon cooling a concentrated solution. Yield: 0.25 g, 45% based on Sb. After $[\text{Et}_4\text{N}]_2[\text{II}]$ was isolated, the solution was concentrated and placed in the freezer, upon which crystals of $[\text{Et}_4\text{N}]_2[\text{Sb}_2\text{Fe}_5(\text{CO})_{17}]$ grew.

- (12) (a) Corbett, J. D. *Prog. Inorg. Chem.* **1976**, *21*, 129. (b) Corbett, J. D. *Chem. Rev.* **1985**, *85*, 383. (c) Schafer, H.; Eisenmann, B.; Müller, W. *Angew. Chem., Int. Ed. Engl.* **1973**, *12*, 694. (d) Schnering, H. G. V. *Angew. Chem., Int. Ed. Engl.* **1981**, *20*, 33–51.
- (13) Etzrodt, G.; Boese, R.; Schmid, G. *Chem. Ber.* **1979**, *112*, 2574.
- (14) Wallis, J.; Müller, G.; Schmidbaur, H. *Inorg. Chem.* **1987**, *26*, 458.
- (15) Wallis, J.; Müller, G.; Schmidbaur, H. *J. Organomet. Chem.* **1987**, *325*, 159.
- (16) Whitmire, K. H.; Leigh, J. S.; Gross, M. *J. Chem. Soc., Chem. Commun.* **1987**, 926.
- (17) Churchill, M. R.; Fettinger, J. C.; Whitmire, K. H. *J. Organomet. Chem.* **1985**, *284*, 13–23.
- (18) Ang, H. G.; Hay, C. M.; Johnson, B. F. G.; Lewis, J.; Raithby, P. R.; Whitton, A. J. *J. Organomet. Chem.* **1987**, *330*, C5–C11.
- (19) Whitmire, K. H.; Lagrone, C. B.; Churchill, M. R.; Fettinger, J. C.; Biondi, L. V. *Inorg. Chem.* **1984**, *23*, 4227.
- (20) Leigh, J. S.; Whitmire, K. H. *Angew. Chem., Int. Ed. Engl.* **1988**, *27*, 396.
- (21) Churchill, M. R.; Fettinger, J. C.; Whitmire, K. H.; Lagrone, C. B. *J. Organomet. Chem.* **1986**, *303*, 99.
- (22) Whitmire, K. H.; Raghuvver, K. S.; Churchill, M. R.; Fettinger, J. C.; See, R. F. *J. Am. Chem. Soc.* **1986**, *108*, 2778.
- (23) Martinengo, S.; Ciani, G. *J. Chem. Soc., Chem. Commun.* **1987**, 1589.
- (24) Whitmire, K. H.; Shieh, M.; Lagrone, C. B.; Robinson, B. H.; Churchill, M. R.; Fettinger, J. C.; See, R. F. *Inorg. Chem.* **1987**, *26*, 2798.
- (25) Vidal, J.; Troup, J. M. *J. Organomet. Chem.* **1981**, *213*, 351.
- (26) Whitmire, K. H.; Leigh, J. S.; Luo, S.-F.; Shieh, M.; Fabiano, M. D. *Nouv. J. Chim.* **1988**, *12*, 397.
- (27) (a) Arif, A. M.; Cowley, A. H.; Pakulski, M. *J. Chem. Soc., Chem. Commun.* **1987**, 662. (b) Rheingold, A. L.; Geib, S. J.; Shieh, M.; Whitmire, K. H. *Inorg. Chem.* **1987**, *26*, 463.
- (28) Cowley, A. H.; Norman, N. C.; Pakulski, M.; Bricker, D. L.; Russell, D. H. *J. Am. Chem. Soc.* **1985**, *107*, 8211.

Table I. Crystallographic Data for $[\text{Et}_4\text{N}]^+$ Salts of I-IV

compd	$[\text{Et}_4\text{N}]_3[\text{I}]$	$[\text{Et}_4\text{N}]_2[\text{II}]$	$[\text{Et}_4\text{N}][\text{III}]$	$[\text{Et}_4\text{N}]_2[\text{IV}]$
formula	$\text{C}_{46}\text{H}_{60}\text{SbFe}_4\text{O}_{16}\text{N}_3$	$\text{C}_{25}\text{H}_{41}\text{SbFe}_4\text{O}_{13}\text{N}_2$	$\text{C}_{21}\text{H}_{22}\text{SbFe}_4\text{O}_{13}\text{N}$	$\text{C}_{28}\text{H}_{40}\text{SbFe}_3\text{ClO}_{12}\text{N}_2$
MW	1184.06	970.79	841.54	921.37
space group	$P2_1/n$ (No. 14)	$P2_1/c$ (No. 14)	$P\bar{1}$ (No. 2)	$C2/c$ (No. 15)
a , Å	13.415 (2)	13.805 (6)	12.714 (2)	29.30 (1)
b , Å	19.601 (2)	18.934 (9)	14.342 (2)	18.500 (6)
c , Å	19.156 (2)	15.295 (6)	8.970 (2)	16.844 (6)
α , deg			99.57 (1)	
β , deg	90.973 (9)	97.76 (3)	105.27 (1)	119.58 (2)
γ , deg			82.34 (1)	
V , Å ³	5036.3 (9)	3961 (3)	1549.0 (4)	7942 (6)
Z	4	4	2	8
ρ_{calcd} , g cm ⁻³	1.56	1.63	1.80	1.54
$\mu(\text{Mo K}\alpha)$, cm ⁻¹	17.58	22.07	27.53	18.72
T , °C	23	23	23	-80
λ , Å			0.710 69	
transm coeff	1.000-0.941	1.000-0.393	1.000-0.876	1.000-0.942
R , %	4.3	4.4	3.6	4.4
R_w , %	5.7	5.8	5.4	6.7

$[\text{Et}_4\text{N}]_2[\text{II}]$ is soluble in CH_2Cl_2 , MeOH, MeCN, and THF but insoluble in hexane, toluene, and Et_2O . IR (CH_2Cl_2 , cm^{-1}): 2030 w, 1966 m, 1945 s, 1920 m. ^1H NMR (in acetone- d_6): δ 1.38 (24, triplet), 3.47 (16, quartet), -19.74 ppm (1, singlet). Anal. Calcd: Sb, 12.54; Fe, 23.01. Found: Sb, 12.37; Fe, 22.26. The crystal used for X-ray diffraction was grown by cooling a concentrated MeOH solution of the compound.

Synthesis of $[\text{Et}_4\text{N}][\text{III}]$. $[\text{Et}_4\text{N}]_2[\text{II}]$ (0.549 g, 0.565 mmol) was weighed in a drybox into a Schlenk flask and then dissolved in CH_2Cl_2 . Trifluoromethanesulfonic acid (0.05 mL, 0.6 mmol) was added, and the color turned reddish brown. The solution was refluxed for 6 h and filtered, and the CH_2Cl_2 was removed under vacuum. The solid residue was extracted with Et_2O until the extract was colorless. All Et_2O extracts were combined, and the solvent was removed under vacuum. The solid residue was dissolved in CH_2Cl_2 . An equal volume of hexane was layered on top of the solution, and black crystals grew upon slow diffusion. Yield: 0.28 g, 60% based on Sb.

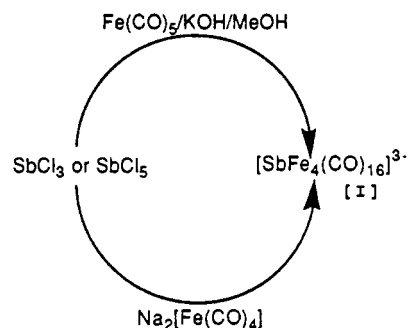
$[\text{Et}_4\text{N}][\text{III}]$ is soluble in Et_2O , CH_2Cl_2 , MeOH, MeCN, and THF but insoluble in hexane and toluene. IR (MeOH, cm^{-1}): 2070 w, 2030 s, 2020 vs, 2000 vs, 1965 m, 1951 m, 1935 m. ^1H NMR (in acetonitrile- d_3): δ 1.19 (6, triplet), 3.14 (4, quartet), -22.63 ppm (1, singlet). Anal. Calcd: Sb, 14.47; Fe, 26.55. Found: Sb, 14.28; Fe, 25.76. The crystal used for X-ray diffraction was grown from a concentrated cooled solution of the compound in CH_2Cl_2 .

Synthesis of $[\text{Et}_4\text{N}][\text{IV}]$. Method 1. Reaction of $[\text{Et}_4\text{N}]_3[\text{I}]$ with $\text{TiCl}_3 \cdot 4\text{H}_2\text{O}$. $\text{TiCl}_3 \cdot 4\text{H}_2\text{O}$ (0.169 g, 0.441 mmol) and $[\text{Et}_4\text{N}]_3[\text{I}]$ (0.527 g, 0.44 mmol) were placed in a Schlenk flask and then dissolved in MeCN. The solution changed from red to reddish brown immediately as a white precipitate developed. The solution was stirred for 20 h and then filtered and the MeCN removed under vacuum. The solid residue was dissolved in CH_2Cl_2 and filtered, and deep red crystals grew upon cooling this concentrated solution. Yield: 0.29 g, 73% based on Sb.

Method 2. Reaction of $[\text{Et}_4\text{N}]_3[\text{I}]$ with SbCl_3 . SbCl_3 (0.102 g, 0.446 mmol) and $[\text{Et}_4\text{N}]_3[\text{I}]$ (0.525 g, 0.446 mmol) were dissolved in MeCN. The red solution turned reddish brown immediately and was stirred overnight. The solution was then filtered, the MeCN removed under vacuum, and the solid residue dissolved in CH_2Cl_2 and filtered. Deep red crystals grew from this concentrated solution upon cooling. Yield: 0.28 g, 69% based on Sb.

$[\text{Et}_4\text{N}]_2[\text{IV}]$ is soluble in CH_2Cl_2 , MeCN, and THF but insoluble in hexane and Et_2O . IR (CH_2Cl_2 , cm^{-1}): 2030 w, 1995 vs, 1915 vs. Anal. Calcd: Fe, 18.18. Found: Fe, 17.16. A crystal suitable for X-ray diffraction grew from its concentrated CH_2Cl_2 solution upon cooling.

X-ray Analysis of $[\text{Et}_4\text{N}]_3[\text{I}]$, $[\text{Et}_4\text{N}]_2[\text{II}]$, $[\text{Et}_4\text{N}][\text{III}]$, and $[\text{Et}_4\text{N}]_2[\text{IV}]$. The crystallographic data collection parameters are tabulated in Table I. Each crystal was mounted on a glass fiber and fixed by epoxy glue. For $[\text{Et}_4\text{N}]_2[\text{IV}]$, X-ray diffraction at room temperature gave broad peaks and the crystal decayed quickly during data collection. The preliminary data set indicated the presence of solvent CH_2Cl_2 that was probably being lost during collection, resulting in crystal decomposition. The data set was recollected on a new crystal at -80 °C, and the decay problems were eliminated. The space groups of $[\text{Et}_4\text{N}]_3[\text{I}]$ and $[\text{Et}_4\text{N}]_2[\text{II}]$ were unambiguously assigned according to systematic absences of diffraction intensity. Space groups $P\bar{1}$ and $P1$ were possible choices for $[\text{Et}_4\text{N}][\text{III}]$ according to the systematic absences; however, the statistically more probable centrosymmetric space group $P\bar{1}$ was chosen and the structure was successfully refined. Systematic absences for $[\text{Et}_4\text{N}]_2[\text{IV}]$ would allow choice of space group Cc (No. 9, acentric) or $C2/c$ (No. 15, centric), but intensity statistics and cell volume sug-

Scheme II. Synthesis of $[\text{Et}_4\text{N}]_3[\text{SbFe}_4(\text{CO})_{16}]$ 

gested the latter centric choice for which successful structure solution and refinement were obtained. For $[\text{Et}_4\text{N}]_2[\text{II}]$ and $[\text{Et}_4\text{N}][\text{III}]$, the ORTEP drawings show that the anion could possess possible mirror symmetry suggestive of a higher symmetry space group. Reexamination of the cell constants using the program TRACER indicated no other cell choice for $[\text{Et}_4\text{N}]_2[\text{II}]$ or $[\text{Et}_4\text{N}][\text{III}]$. Upon greatly increasing the error limits on the TRACER search, we could obtain a monoclinic C-centered cell for $[\text{Et}_4\text{N}][\text{III}]$; however, the increase in the data error and the significant deviation in volume of the unit cell versus that of double the original triclinic choice [2862 vs 2(1549) Å³] make that possibility seem unreasonable. Furthermore, the least-squares cycles showed no unusually large correlation coefficients ascribable to misassigned symmetry, nor were there apparent problems with the thermal ellipsoids that could indicate such an error. Examination of the cations in relationship to the anion showed that addition of a mirror plane to the anions could not be accommodated by the cations. We concluded, therefore, that while the cluster anions have near mirror symmetry, this symmetry cannot be crystallographic due to the positioning of the cations in the unit cell. For $[\text{Et}_4\text{N}]_3[\text{I}]$, atomic coordinates of the Bi analogue, $[\text{Et}_4\text{N}]_3[\text{BiFe}_4(\text{CO})_{16}]$,²¹ were used for structure solution, as the two compounds are isomorphous. For the other three compounds, the program MITHRIL²⁹ was used to locate Sb and Fe atoms. Following refinements used the TEXSAN(2.0) structure solution package (Molecular Structure Corp.), and all non-hydrogen atoms were located. The two bridging H ligands in $[\text{Et}_4\text{N}][\text{III}]$ were found from electron density maps and refined. All non-hydrogen atoms were refined anisotropically until convergence. The disorder of the $[\text{Et}_4\text{N}]^+$ cations in $[\text{Et}_4\text{N}]_3[\text{I}]$ was resolvable into two distinct sets and treated as previously done for $[\text{Et}_4\text{N}]_3[\text{BiFe}_4(\text{CO})_{16}]$.²¹

Results

Synthesis of $[\text{Et}_4\text{N}]_3[\text{I}]$, $[\text{Et}_4\text{N}]_2[\text{II}]$, $[\text{Et}_4\text{N}][\text{III}]$, and $[\text{Et}_4\text{N}]_2[\text{IV}]$. There are four different but related methods to prepare $[\text{Et}_4\text{N}]_3[\text{I}]$ (see Scheme II). The reaction of $\text{Na}_2[\text{Fe}(\text{CO})_4]$ in MeCN, or $\text{Fe}(\text{CO})_5$ in methanolic KOH, with antimony halides proceeds to the same product, $[\text{Et}_4\text{N}]_3[\text{SbFe}_4(\text{CO})_{16}]$, all with approximately the same yield. The choice of SbCl_3 or SbCl_5 did not make a dramatic impact upon reactions although the order of addition of SbCl_3 was important in the $\text{Fe}(\text{CO})_5/\text{MeOH}/\text{KOH}$ system.

(29) Gilmore, G. J. "MITHRIL: A Computer Program for the Automatic Solution of Crystal Structures from X-Ray Data", University of Glasgow, Scotland, 1983.

Table II. Selected Positional Parameters and $B(\text{eq})$ for $[\text{Et}_4\text{N}]_3[\text{I}]$

atom	<i>x</i>	<i>y</i>	<i>z</i>	$B(\text{eq}), \text{\AA}^2$
Sb1	-0.01442 (3)	0.24890 (3)	0.22846 (2)	2.71 (2)
Fe1	-0.20035 (7)	0.28765 (5)	0.19631 (5)	3.36 (4)
Fe2	0.09807 (7)	0.25122 (5)	0.11548 (5)	3.49 (4)
Fe3	0.06177 (7)	0.33422 (5)	0.32380 (5)	3.29 (4)
Fe4	-0.01457 (7)	0.12346 (5)	0.28238 (5)	3.40 (4)
O11	-0.1368 (5)	0.4298 (3)	0.2079 (4)	7.7 (4)
O12	-0.2699 (4)	0.2105 (4)	0.3156 (3)	6.6 (3)
O13	-0.1889 (5)	0.2174 (4)	0.0617 (3)	7.7 (4)
O14	-0.4025 (4)	0.3353 (3)	0.1748 (3)	6.5 (3)
O21	0.0418 (5)	0.1101 (3)	0.0889 (3)	6.7 (4)
O22	-0.0138 (5)	0.3695 (3)	0.0664 (4)	7.3 (4)
O23	0.2763 (4)	0.2693 (3)	0.2026 (3)	6.3 (3)
O24	0.2123 (5)	0.2532 (4)	-0.0113 (3)	7.8 (4)
O31	0.1047 (5)	0.4301 (3)	0.2124 (3)	6.3 (3)
O32	0.2074 (5)	0.2296 (3)	0.3632 (3)	6.5 (3)
O33	-0.1314 (4)	0.3374 (3)	0.3915 (3)	5.9 (3)
O34	0.1369 (4)	0.4233 (3)	0.4323 (3)	6.2 (3)
O41	-0.0691 (5)	0.1819 (3)	0.4170 (3)	6.0 (3)
O42	-0.1631 (5)	0.0892 (3)	0.1756 (4)	8.0 (4)
O43	0.1963 (4)	0.1096 (3)	0.2494 (3)	6.3 (3)
O44	-0.0305 (6)	-0.0105 (3)	0.3457 (4)	8.0 (4)
C11	-0.1556 (6)	0.3279 (4)	0.2039 (4)	4.7 (4)
C12	-0.2370 (5)	0.2399 (4)	0.2699 (4)	4.3 (3)
C13	-0.1899 (5)	0.2452 (4)	0.1159 (4)	4.5 (3)
C14	-0.3214 (5)	0.3156 (4)	0.1809 (4)	4.0 (3)
C21	0.0599 (6)	0.1663 (3)	0.1013 (4)	4.5 (4)
C22	0.0273 (6)	0.3217 (4)	0.0886 (4)	4.7 (4)
C23	0.2040 (6)	0.2627 (4)	0.1719 (4)	4.4 (4)
C24	0.1666 (6)	0.2523 (4)	0.0399 (4)	4.8 (4)
C31	0.0867 (6)	0.3898 (4)	0.2537 (4)	4.1 (4)
C32	0.1475 (6)	0.2693 (4)	0.3452 (4)	4.3 (4)
C33	-0.0572 (6)	0.3337 (4)	0.3622 (4)	4.0 (3)
C34	0.1067 (5)	0.3881 (4)	0.3884 (4)	4.4 (4)
C41	-0.0471 (6)	0.1621 (4)	0.3623 (4)	4.2 (4)
C42	-0.1048 (6)	0.1051 (4)	0.2167 (4)	4.8 (4)
C43	0.1129 (6)	0.1178 (4)	0.2623 (4)	4.4 (4)
C44	-0.0229 (6)	0.0428 (4)	0.3194 (4)	4.8 (4)

When SbCl_5 and MeOH were mixed prior to reaction, the product isolated was $[\text{Et}_4\text{N}]_2[\text{III}]$. This probably occurs via the initial hydrolysis of SbCl_5 to produce HCl , which can then protonate $[\text{Et}_4\text{N}]_3[\text{SbFe}_4(\text{CO})_{16}]$. This reaction is known to give the hydride compound (vide infra). If the SbCl_5 was added directly to a MeOH solution of $\text{Fe}(\text{CO})_5/\text{KOH}$, then some $[\text{Et}_4\text{N}]_2[\text{II}]$ was obtained, but the major product was $[\text{Et}_4\text{N}]_3[\text{I}]$. Varying amounts of $[\text{Et}_4\text{N}]_2[\text{ClSbFe}_3(\text{CO})_{12}]$ were sometimes obtained as a by-product of these reactions. Compound $[\text{I}]^{3-}$ as its $[\text{Et}_4\text{N}]^+$ salt is not soluble in organic solvents except MeCN and THF . The infrared spectrum in MeCN shows three bands consistent with T_d symmetry in solution and also nearly identical with that seen for $[\text{Et}_4\text{N}]_3[\text{BiFe}_4(\text{CO})_{16}]$.^{19,21}

Protonation of $[\text{Et}_4\text{N}]_3[\text{I}]$ with 1 equiv of trifluoromethanesulfonic acid gave as the major product $[\text{Et}_4\text{N}]_2[\text{III}]$, which is accompanied by a small amount of $[\text{Et}_4\text{N}]_2[\text{Sb}_2\text{Fe}_5(\text{CO})_{17}]$, whose structure has been reported.²⁶ The first product can be thought of as arising from a simple protonation-induced metal-metal bond-formation process, while the second derives from a formal cluster oxidation. Surprisingly, addition of 2 equiv of trifluoromethanesulfonic acid directly to $[\text{Et}_4\text{N}]_3[\text{I}]$ yielded primarily $[\text{Et}_4\text{N}]_2[\text{Sb}_2\text{Fe}_5(\text{CO})_{17}]$ with a trace amount of $[\text{Et}_4\text{N}]_2[\text{III}]$, while addition of a second equivalent of trifluoromethanesulfonic acid to $[\text{Et}_4\text{N}]_2[\text{II}]$ produced mainly pure $[\text{Et}_4\text{N}][\text{III}]$.

A very facile reaction of $[\text{Et}_4\text{N}]_3[\text{I}]$ occurs with 1 equiv of $\text{TiCl}_3 \cdot 4\text{H}_2\text{O}$ or SbCl_3 to give $[\text{Et}_4\text{N}]_2[\text{IV}]$. This can be viewed as a formal replacement of a $[\text{Fe}(\text{CO})_4]^{2-}$ group by Cl^- . However, the direct replacement with halides of nonoxidizing capability such as $[\text{Et}_4\text{N}]^+\text{X}^-$ or $[\text{PPN}]^+\text{X}^-$ does not occur.

Crystal Structure of $[\text{Et}_4\text{N}]_3[\text{I}]$. The crystal structure of $[\text{Et}_4\text{N}]_3[\text{I}]$ contains ordered anions $[\text{SbFe}_4(\text{CO})_{16}]^{3-}$ and disordered $[\text{Et}_4\text{N}]^+$ cations in the ratio of 1:3. Atomic positional parameters are provided in Table II, while selected bond distances and angles are found in Table VI. The structure of the anion (see Figure 1) has an Sb atom that is tetrahedrally bound to four

Table III. Selected Positional Parameters and $B(\text{eq})$ for $[\text{Et}_4\text{N}]_2[\text{III}]$

atom	<i>x</i>	<i>y</i>	<i>z</i>	$B(\text{eq}), \text{\AA}^2$
Sb1	0.71796 (4)	0.05710 (3)	0.79336 (3)	3.89 (2)
Fe1	0.81984 (9)	-0.05070 (6)	0.79857 (7)	4.42 (5)
Fe2	0.89444 (9)	0.08207 (6)	0.81263 (8)	4.60 (6)
Fe3	0.79177 (1)	0.04076 (6)	0.65652 (7)	4.69 (6)
Fe4	0.55712 (9)	0.09185 (7)	0.84176 (8)	4.81 (6)
O11	0.8228 (6)	-0.0621 (4)	0.9883 (5)	8.1 (4)
O12	1.0020 (5)	-0.1211 (4)	0.7736 (6)	8.7 (5)
O13	0.6729 (5)	-0.1584 (4)	0.7524 (5)	8.6 (5)
O21	0.9342 (6)	0.0979 (6)	1.0028 (5)	10.7 (6)
O22	0.8886 (7)	0.2316 (4)	0.7701 (8)	12.1 (6)
O23	1.0913 (6)	0.0454 (5)	0.7835 (6)	9.6 (5)
O31	0.6406 (6)	-0.0277 (5)	0.5361 (6)	10.4 (5)
O32	0.7379 (8)	0.1806 (5)	0.5938 (6)	11.7 (6)
O33	0.9729 (6)	0.0284 (6)	0.5812 (5)	12.1 (6)
O41	0.3626 (7)	0.1255 (6)	0.8824 (6)	12.1 (6)
O42	0.5681 (6)	-0.0427 (4)	0.9361 (5)	8.6 (5)
O43	0.4841 (6)	0.1007 (5)	0.6548 (5)	10.1 (5)
O44	0.6605 (8)	0.2081 (4)	0.9402 (5)	11.2 (6)
C11	0.8215 (7)	-0.0569 (5)	0.9138 (7)	5.9 (5)
C12	0.9319 (7)	-0.0930 (5)	0.7843 (6)	5.8 (5)
C13	0.7306 (7)	-0.1145 (6)	0.7708 (6)	5.8 (5)
C21	0.9162 (8)	0.0904 (7)	0.9275 (8)	7.3 (6)
C22	0.8888 (7)	0.1726 (6)	0.7847 (8)	6.9 (6)
C23	1.0124 (7)	0.0586 (5)	0.7925 (7)	6.3 (5)
C31	0.7003 (8)	-0.0003 (6)	0.5856 (7)	7.0 (6)
C32	0.7599 (8)	0.1264 (6)	0.6198 (6)	6.9 (5)
C33	0.9012 (8)	0.0320 (6)	0.6118 (6)	6.9 (6)
C41	0.4403 (8)	0.1116 (6)	0.8687 (7)	8.1 (6)
C42	0.5642 (7)	0.0110 (5)	0.8977 (6)	5.7 (5)
C43	0.5134 (7)	0.0974 (6)	0.7296 (7)	6.3 (5)
C44	0.619 (1)	0.1623 (6)	0.9014 (6)	7.4 (6)

Table IV. Selected Positional Parameters and $B(\text{eq})$ for $[\text{Et}_4\text{N}][\text{III}]$

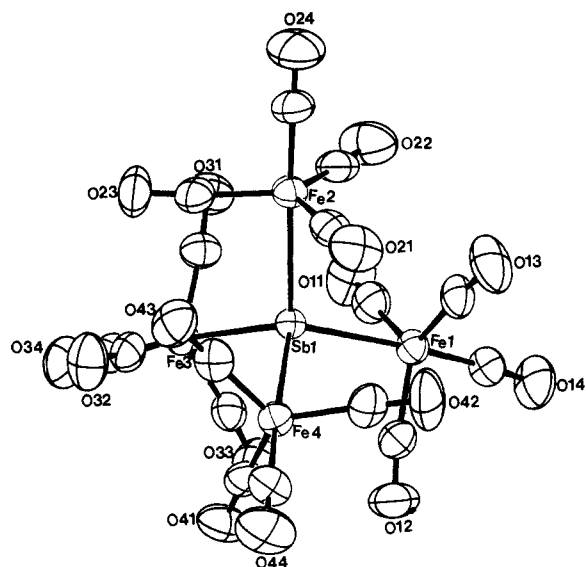
atom	<i>x</i>	<i>y</i>	<i>z</i>	$B(\text{eq}), \text{\AA}^2$
Sb1	0.77638 (2)	0.71774 (2)	0.25810 (3)	3.12 (1)
Fe1	0.76689 (5)	0.70234 (4)	-0.02208 (7)	3.71 (2)
Fe2	0.78895 (4)	0.54712 (4)	0.13719 (6)	3.34 (2)
Fe3	0.59845 (4)	0.66944 (4)	0.09314 (7)	3.50 (2)
Fe4	0.85454 (4)	0.81430 (4)	0.51413 (6)	3.13 (2)
O11	0.6570 (5)	0.6408 (4)	-0.3468 (5)	9.3 (3)
O12	0.7149 (4)	0.9054 (3)	-0.0199 (6)	8.0 (2)
O13	0.9934 (3)	0.7127 (3)	-0.0279 (5)	7.1 (2)
O21	0.7774 (4)	0.4861 (3)	0.4267 (4)	6.5 (2)
O22	0.7431 (3)	0.3666 (3)	-0.0649 (5)	6.9 (2)
O23	1.0278 (3)	0.5244 (3)	0.2010 (5)	6.0 (2)
O31	0.4528 (3)	0.5985 (3)	-0.2029 (5)	6.8 (2)
O32	0.4998 (3)	0.8631 (3)	0.0963 (5)	6.7 (2)
O33	0.4890 (3)	0.6273 (3)	0.3184 (5)	7.3 (2)
O41	0.9396 (4)	0.9277 (3)	0.8122 (5)	8.0 (2)
O42	0.9801 (4)	0.6390 (3)	0.6146 (5)	7.1 (2)
O43	0.9489 (3)	0.9244 (3)	0.3421 (5)	5.9 (2)
O44	0.6286 (3)	0.8620 (3)	0.5445 (5)	6.8 (2)
C11	0.6998 (5)	0.6646 (4)	-0.2214 (6)	5.5 (2)
C12	0.7336 (4)	0.8260 (4)	-0.0214 (6)	5.4 (2)
C13	0.9045 (4)	0.7080 (4)	-0.0281 (6)	5.0 (2)
C21	0.7818 (4)	0.5108 (3)	0.3146 (6)	4.5 (2)
C22	0.7623 (4)	0.4367 (3)	0.0104 (6)	4.6 (2)
C23	0.9358 (4)	0.5333 (3)	0.1798 (5)	4.2 (2)
C31	0.5126 (4)	0.6246 (3)	-0.0895 (6)	4.4 (2)
C32	0.5410 (3)	0.7874 (3)	0.0949 (5)	4.4 (2)
C33	0.5335 (4)	0.6427 (3)	0.2336 (6)	4.9 (2)
C41	0.9079 (4)	0.8830 (4)	0.6976 (6)	5.1 (2)
C42	0.9306 (4)	0.7069 (3)	0.5767 (5)	4.5 (2)
C43	0.9104 (3)	0.8807 (3)	0.4079 (5)	3.9 (2)
C44	0.7174 (4)	0.8413 (3)	0.5330 (5)	4.4 (2)
H1	0.780 (4)	0.589 (3)	-0.034 (5)	5 (1)
H2	0.661 (4)	0.563 (4)	0.040 (6)	6 (1)

$\text{Fe}(\text{CO})_4$ units. The average Sb-Fe bond distance is 2.666 (3) \AA . All Fe atoms have a trigonal-bipyramidal coordination geometry, with the Sb atom occupying an axial position.

Crystal Structure of $[\text{Et}_4\text{N}]_2[\text{III}]$. The crystal structure of $[\text{Et}_4\text{N}]_2[\text{III}]$ contains ordered $[\text{HSbFe}_4(\text{CO})_{13}]^{2-}$ anions and ordered $[\text{Et}_4\text{N}]^+$ cations in the ratio 1:2. Atomic positional parameters are given in Table III, and selected bond distances and

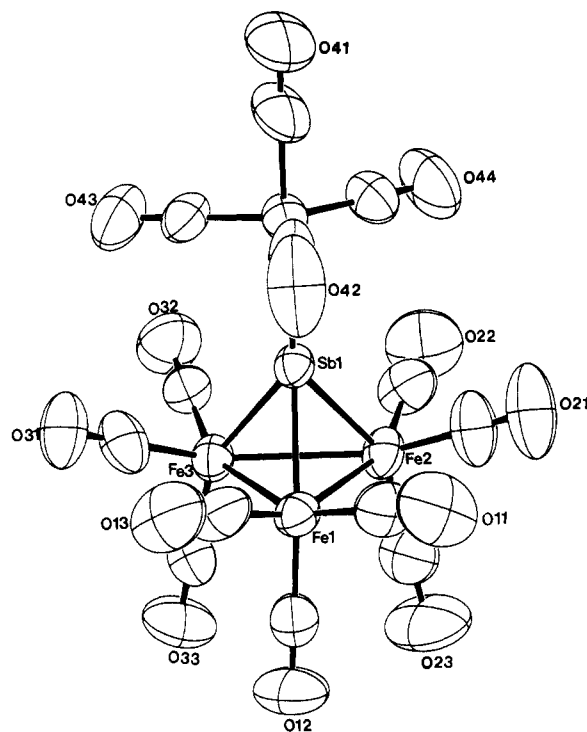
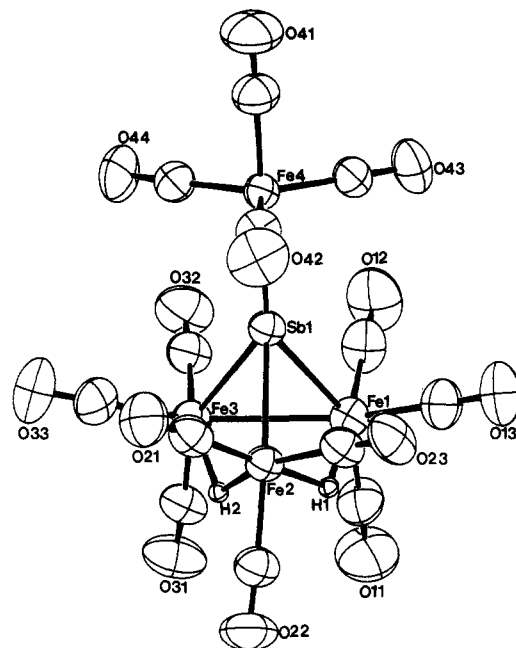
Table V. Positional Parameters and $B(\text{eq})$ for $[\text{Et}_4\text{N}]_2[\text{IV}]$

atom	x	y	z	$B(\text{eq}), \text{\AA}^2$
Sb1	0.12084 (2)	0.27160 (3)	0.12503 (4)	2.32 (2)
Fe1	0.12968 (5)	0.23384 (7)	0.27845 (9)	2.81 (5)
Fe2	0.03248 (5)	0.32465 (7)	0.00415 (9)	2.83 (5)
Fe3	0.16175 (5)	0.18226 (7)	0.06163 (9)	2.73 (5)
C11	0.1792 (1)	0.3788 (1)	0.1695 (2)	3.38 (9)
O11	0.1386 (4)	0.1944 (5)	0.4524 (5)	6.1 (4)
O12	0.1015 (4)	0.0870 (4)	0.2044 (7)	6.4 (4)
O13	0.2430 (3)	0.2694 (5)	0.3688 (6)	5.7 (4)
O14	0.0484 (3)	0.3403 (5)	0.2418 (5)	4.7 (3)
O21	-0.0680 (3)	0.3668 (5)	-0.1525 (2)	5.4 (4)
O22	0.0578 (3)	0.4638 (4)	0.0995 (6)	5.4 (4)
O23	0.0647 (3)	0.3017 (5)	-0.1327 (5)	5.8 (4)
O24	-0.0165 (3)	0.2243 (5)	0.0748 (5)	6.0 (4)
O31	0.1999 (4)	0.0799 (5)	-0.0236 (5)	6.6 (4)
O32	0.0562 (3)	0.1189 (4)	-0.0391 (6)	5.5 (4)
O33	0.1933 (3)	0.3071 (4)	-0.0093 (6)	5.5 (4)
O34	0.2332 (3)	0.1238 (5)	0.2425 (5)	5.7 (4)
C11	0.1349 (4)	0.2098 (6)	0.3829 (7)	3.9 (4)
C12	0.1132 (5)	0.1469 (6)	0.2331 (8)	4.1 (5)
C13	0.1982 (2)	0.2564 (6)	0.3311 (7)	4.1 (4)
C14	0.0807 (4)	0.2979 (6)	0.2555 (6)	3.2 (4)
C21	-0.0289 (4)	0.3513 (6)	-0.0894 (7)	3.6 (4)
C22	0.0488 (4)	0.4093 (5)	0.0642 (7)	3.4 (4)
C23	0.0542 (4)	0.3095 (6)	-0.0766 (7)	3.8 (4)
C24	0.0034 (4)	0.2630 (6)	0.0479 (7)	3.9 (4)
C31	0.1845 (4)	0.1206 (6)	0.0120 (7)	3.9 (4)
C32	0.0994 (4)	0.1465 (5)	0.0032 (7)	3.6 (4)
C33	0.1788 (4)	0.2584 (6)	0.0190 (7)	3.9 (4)
C34	0.2048 (4)	0.1495 (6)	0.1727 (7)	3.7 (4)

**Figure 1.** ORTEP diagram of $[\text{SbFe}_4(\text{CO})_{16}]^{3-}$ ($[\text{I}]^{3-}$), showing 50% thermal probability ellipsoids and atom labeling. The carbonyl C atoms are left unlabeled for clarity. Their numbering is the same as that of the oxygen atoms to which they are attached. Important bond distances and angles are listed in Table VI.

angles are listed in Table VII. The anion (see Figure 2) has a SbFe_3 tetrahedral core with an external $\text{Fe}(\text{CO})_4$ group attached to the Sb atom. The average Sb–Fe bond distance within the tetrahedral core is 2.467 (7) \AA , while the Sb–Fe distance to the isolated $\text{Fe}(\text{CO})_4$ group is longer [2.521 (2) \AA]. The H ligand, which was not located directly, apparently bridges Fe1–Fe3, as indicated by inspection of the bonding parameters: the Fe1–Fe3 bond distance [2.764 (2) \AA] is slightly longer than those of Fe1–Fe2 [2.714 (2) \AA] and Fe2–Fe3 [2.722 (2) \AA], and the bond angles of C12–Fe1–Fe3 [102.6 (3) $^\circ$] and C33–Fe3–Fe1 [102.1 (3) $^\circ$] are larger than those of C12–Fe1–Fe2 [95.7 (3) $^\circ$] and C33–Fe3–Fe2 [89.7 (3) $^\circ$].

Crystal Structure of $[\text{Et}_4\text{N}][\text{III}]$. The crystal structure of $[\text{Et}_4\text{N}][\text{III}]$ contains ordered $[\text{H}_2\text{SbFe}_4(\text{CO})_{13}]^-$ anions and ordered $[\text{Et}_4\text{N}]^+$ cations in the ratio of 1:1. Atomic positional parameters are given in Table VI. Selected bond distances and

**Figure 2.** ORTEP diagram of $[\text{HSbFe}_4(\text{CO})_{13}]^{2-}$ ($[\text{II}]^{2-}$), showing 50% thermal probability ellipsoids and atom labeling. The carbonyl C atoms are left unlabeled for clarity. Their numbering is the same as that of the oxygen atoms to which they are attached. Important bond distances and angles are listed in Table VII.**Figure 3.** ORTEP diagram of $[\text{H}_2\text{SbFe}_4(\text{CO})_{13}]^-$ ($[\text{III}]^-$), showing 50% thermal probability ellipsoids and atom labeling. The carbonyl C atoms are left unlabeled for clarity. Their numbering is the same as that of the oxygen atoms to which they are attached. Important bond distances and angles are listed in Table VIII.

angles are given in Table VIII. The anion structure (see Figure 3) is virtually identical with that of $[\text{II}]^{2-}$. The Sb atom caps an Fe_3 triangle to form a tetrahedron, and an external $\text{Fe}(\text{CO})_4$ group is attached to it. The average Sb–Fe distance within the SbFe_3 core is 2.479 (26) \AA , while the Sb–Fe distance to the isolated $\text{Fe}(\text{CO})_4$ group is again longer [2.5073 (8) \AA]; however, one of the Sb–Fe bonds within the cluster is also long [Sb1–Fe2 = 2.5088 (7) \AA]. This lengthening probably arises from the influence of the H ligands, both of which are bound to Fe2, whereas the other

Table VI. Selected Bond Distances and Angles of $[\text{Et}_4\text{N}]_3[\text{I}]$

(a) Bond Distances (Å)			
Sb1-Fe1	2.670 (1)	Fe4-C43	1.763 (8)
Sb1-Fe2	2.663 (1)	Fe4-C44	1.738 (8)
Sb1-Fe3	2.665 (1)	C11-O11	1.145 (9)
Sb1-Fe4	2.666 (1)	C12-O12	1.142 (8)
Fe1-C11	1.781 (9)	C13-O13	1.173 (8)
Fe1-C12	1.770 (8)	C14-O14	1.159 (8)
Fe1-C13	1.758 (8)	C21-O21	1.154 (9)
Fe1-C14	1.734 (7)	C22-O22	1.164 (9)
Fe2-C21	1.760 (9)	C23-O23	1.133 (8)
Fe2-C22	1.748 (9)	C24-O24	1.166 (8)
Fe2-C33	1.785 (8)	C31-O31	1.147 (8)
Fe2-C24	1.728 (7)	C32-O32	1.167 (9)
Fe3-C31	1.766 (8)	C33-O33	1.152 (8)
Fe3-C32	1.759 (8)	C34-O34	1.156 (8)
Fe3-C33	1.769 (8)	C41-O41	1.160 (9)
Fe3-C34	1.728 (8)	C42-O42	1.144 (9)
Fe4-C41	1.770 (9)	C43-O43	1.161 (9)
Fe4-C42	1.768 (8)	C44-O44	1.164 (9)

(b) Bond Angles (deg)			
Fe1-Sb1-Fe2	110.27 (3)	C32-Fe3-C33	119.4 (3)
Fe1-Sb1-Fe3	109.03 (3)	C32-Fe3-C34	93.2 (3)
Fe1-Sb1-Fe4	110.19 (3)	C33-Fe3-Sb1	86.7 (2)
Fe2-Sb1-Fe3	109.27 (3)	C33-Fe3-C34	90.6 (3)
Fe2-Sb1-Fe4	109.53 (3)	C34-Fe3-Sb1	177.1 (3)
Fe3-Sb1-Fe4	108.51 (3)	C41-Fe4-Sb1	86.7 (2)
C11-Fe1-Sb1	86.3 (2)	C41-Fe4-C42	121.8 (4)
C11-Fe1-C12	122.0 (4)	C41-Fe4-C43	118.1 (4)
C11-Fe1-C13	119.0 (4)	C41-Fe4-C44	91.0 (3)
C11-Fe1-C14	91.8 (3)	C42-Fe4-Sb1	85.3 (2)
C12-Fe1-Sb1	86.3 (2)	C42-Fe4-C43	119.1 (4)
C12-Fe1-C13	118.4 (4)	C42-Fe4-C44	93.3 (4)
C12-Fe1-C14	91.8 (3)	C43-Fe4-Sb1	88.1 (2)
C13-Fe1-Sb1	88.9 (2)	C43-Fe4-C44	95.8 (4)
C13-Fe1-C14	95.1 (3)	C44-Fe4-Sb1	176.0 (3)
C14-Fe1-Sb1	176.0 (2)	O11-C11-Fe1	173.1 (7)
C21-Fe2-Sb1	86.7 (2)	O12-C12-Fe1	173.4 (7)
C21-Fe2-C22	123.1 (4)	O13-C13-Fe1	176.1 (7)
C21-Fe2-C23	116.1 (4)	O14-C14-Fe1	175.9 (7)
C21-Fe2-C24	92.3 (4)	O21-C21-Fe2	174.5 (7)
C22-Fe2-Sb1	86.6 (2)	O22-C22-Fe2	174.2 (7)
C22-Fe2-C23	120.1 (4)	O23-C23-Fe2	173.8 (7)
C22-Fe2-C24	92.1 (4)	O24-C24-Fe2	179.6 (9)
C23-Fe2-Sb1	88.0 (2)	O31-C31-Fe3	174.1 (7)
C23-Fe2-C24	94.4 (3)	O32-C32-Fe3	174.7 (7)
C24-Fe2-Sb1	177.6 (3)	O33-C33-Fe3	174.0 (6)
C31-Fe3-Sb1	86.7 (2)	O34-C34-Fe3	179.1 (7)
C31-Fe3-C32	119.4 (3)	O41-C41-Fe4	174.3 (7)
C31-Fe3-C33	120.3 (3)	O42-C42-Fe4	175.8 (7)
C31-Fe3-C34	95.8 (4)	O43-C43-Fe4	175.6 (7)
C32-Fe3-Sb1	86.9 (2)	O44-C44-Fe4	178.0 (8)

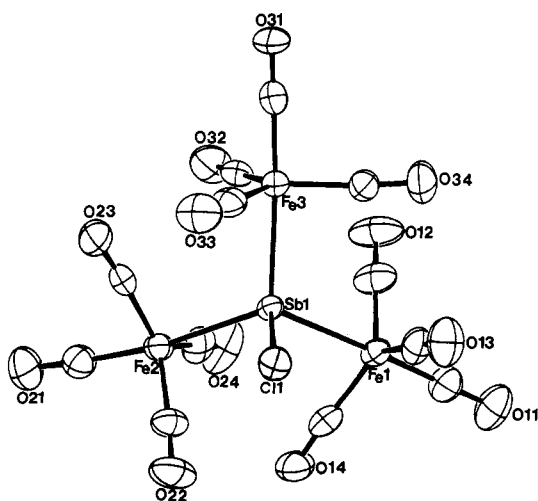


Figure 4. ORTEP diagram of $[\text{ClSbFe}_3(\text{CO})_{12}]^{2-}$ ($[\text{IV}]^{2-}$), showing 50% thermal probability ellipsoids and atom labeling. The carbonyl C atoms are left unlabeled for clarity. Their numbering is the same as that of the oxygen atoms to which they are attached. Important bond distances and angles are listed in Table IX.

Table VII. Selected Bond Distances and Angles of $[\text{Et}_4\text{N}]_2[\text{II}]$

(a) Bond Distances (Å)			
Sb1-Fe1	2.474 (2)	Fe4-C42	1.75 (1)
Sb1-Fe2	2.460 (2)	Fe4-C43	1.74 (1)
Sb1-Fe3	2.467 (2)	Fe4-C44	1.77 (1)
Sb1-Fe4	2.521 (2)	C11-O11	1.14 (1)
Fe1-Fe2	2.714 (2)	C12-O12	1.14 (1)
Fe1-Fe3	2.764 (2)	C13-O13	1.16 (1)
Fe1-C11	1.76 (1)	C21-O21	1.15 (1)
Fe1-C12	1.78 (1)	C22-O22	1.14 (1)
Fe1-C13	1.74 (1)	C23-O23	1.14 (1)
Fe2-Fe3	2.722 (2)	C31-O31	1.16 (1)
Fe2-C21	1.75 (1)	C32-O32	1.13 (1)
Fe2-C22	1.77 (1)	C33-O33	1.15 (1)
Fe2-C23	1.75 (1)	C41-O41	1.15 (1)
Fe3-C31	1.73 (1)	C42-O42	1.17 (1)
Fe3-C32	1.75 (1)	C43-O43	1.16 (1)
Fe3-C33	1.75 (1)	C44-O44	1.16 (1)
Fe4-C41	1.76 (1)		

(b) Bond Angles (deg)			
Fe1-Sb1-Fe2	66.75 (5)	Sb1-Fe3-Fe2	56.34 (4)
Fe1-Sb1-Fe3	68.04 (4)	Fe1-Fe3-Fe2	59.29 (5)
Fe1-Sb1-Fe4	136.50 (5)	C31-Fe3-Sb1	103.8 (3)
Fe2-Sb1-Fe3	67.07 (5)	C31-Fe3-Fe1	103.0 (4)
Fe2-Sb1-Fe4	144.29 (5)	C31-Fe3-Fe2	158.0 (3)
Fe3-Sb1-Fe4	139.68 (5)	C31-Fe3-C32	94.9 (5)
Sb1-Fe1-Fe2	56.38 (5)	C31-Fe3-C33	107.9 (5)
Sb1-Fe1-Fe3	56.38 (5)	C32-Fe3-Sb1	92.4 (3)
Fe2-Fe1-Fe3	59.58 (5)	C32-Fe3-Fe1	146.5 (3)
C11-Fe1-Sb1	91.0 (3)	C32-Fe3-Fe2	95.4 (3)
C11-Fe1-Fe2	91.6 (3)	C32-Fe3-C33	98.9 (5)
C11-Fe1-Fe3	144.0 (3)	C33-Fe3-Sb1	145.2 (3)
C11-Fe1-C12	101.4 (4)	C33-Fe3-Fe1	102.1 (3)
C11-Fe1-C13	96.4 (4)	C33-Fe3-Fe2	89.7 (3)
C12-Fe1-Sb1	150.1 (3)	Sb1-Fe4-C41	175.4 (4)
C12-Fe1-Fe2	95.7 (3)	Sb1-Fe4-C42	85.5 (3)
C12-Fe1-Fe3	102.6 (3)	Sb1-Fe4-C43	85.9 (3)
C12-Fe1-C13	104.8 (4)	Sb1-Fe4-C44	87.9 (4)
C13-Fe1-Sb1	100.3 (3)	C41-Fe4-C42	93.7 (5)
C13-Fe1-Fe2	155.9 (3)	C41-Fe4-C43	90.7 (5)
C13-Fe1-Fe3	102.9 (3)	C41-Fe4-C44	96.6 (6)
Sb1-Fe2-Fe1	56.87 (4)	C42-Fe4-C43	121.5 (5)
Sb1-Fe2-Fe3	56.59 (5)	C42-Fe4-C44	114.6 (5)
Fe1-Fe2-Fe3	61.13 (4)	C43-Fe4-C44	122.7 (5)
C21-Fe2-Sb1	99.8 (3)	Fe1-C11-O11	178.8 (8)
C21-Fe2-Fe1	100.1 (4)	Fe1-C12-O12	178.2 (9)
C21-Fe2-Fe3	154.9 (3)	Fe1-C13-O13	178 (1)
C21-Fe2-C22	98.7 (6)	Fe2-C21-O21	177 (1)
C21-Fe2-C23	99.3 (5)	Fe2-C22-O22	177 (1)
C22-Fe2-Sb1	98.4 (3)	Fe2-C23-O23	176 (1)
C22-Fe2-Fe1	151.2 (3)	Fe3-C31-O31	178 (1)
C22-Fe2-Fe3	93.8 (4)	Fe3-C32-O32	178 (1)
C22-Fe2-C23	102.4 (5)	Fe3-C33-O33	178 (1)
C23-Fe2-Sb1	149.1 (3)	Fe4-C41-O41	177 (1)
C23-Fe2-Fe1	95.9 (3)	Fe4-C42-O42	178.9 (8)
C23-Fe2-Fe3	99.2 (3)	Fe4-C43-O43	180 (1)
Sb1-Fe3-Fe1	56.10 (4)	Fe4-C44-O44	180 (1)

two Fe atoms are bound to only one hydride. The two H ligands were located crystallographically between Fe1-Fe2 and Fe2-Fe3 and refined.

Crystal Structure of $[\text{Et}_4\text{N}]_2[\text{IV}]$. The crystal structure of $[\text{Et}_4\text{N}]_2[\text{IV}]$ contains ordered $[\text{ClSbFe}_3(\text{CO})_{12}]^{2-}$ anions and ordered $[\text{Et}_4\text{N}]^+$ cations in the ratio of 1:2. Atomic positional parameters are given in Table V. Selected bond distances and angles are provided in Table IX. The anion structure (see Figure 4) is virtually the same as that of $[\text{I}]^{2-}$ except one $[\text{Fe}(\text{CO})_4]^{2-}$ group is replaced by Cl^- . Within the anion, the Sb-Cl distance is 2.480 (2) Å and the average Sb-Fe distance is 2.565 (4) Å. As in $[\text{Et}_4\text{N}]_3[\text{I}]$, the Sb atom occupies the axial position on the trigonal-bipyramidal Fe atoms.

Discussion

Crystal Structures of $[\text{Et}_4\text{N}]_3[\text{I}]$, $[\text{Et}_4\text{N}]_2[\text{II}]$, $[\text{Et}_4\text{N}][\text{III}]$, and $[\text{Et}_4\text{N}]_2[\text{IV}]$. In compound $[\text{Et}_4\text{N}]_3[\text{I}]$, the average Sb-Fe bond distance [2.666 (3) Å] is long compared to 2.523 (32) Å in $\text{Sb}_2\text{Fe}_6(\text{CO})_{22}$,²⁷ 2.494 (28) Å in $[\text{Et}_4\text{N}][\text{SbFe}_4(\text{CO})_{14}]$,²⁶ and

Table VIII. Selected Bond Distances and Angles of [Et₄N][III]

(a) Bond Distances (Å)			
Sb1-Fe1	2.4581 (8)	Fe3-C33	1.792 (5)
Sb1-Fe2	2.5088 (7)	Fe4-C41	1.786 (5)
Sb1-Fe3	2.4700 (8)	Fe4-C42	1.796 (4)
Sb1-Fe4	2.5073 (8)	Fe4-C43	1.777 (4)
Fe1-Fe2	2.7849 (9)	Fe4-C44	1.781 (4)
Fe1-Fe3	2.7340 (9)	O11-C11	1.130 (6)
Fe1-H1	1.60 (5)	O12-C12	1.129 (6)
Fe1-C11	1.793 (5)	O13-C13	1.140 (6)
Fe1-C12	1.768 (5)	O21-C21	1.137 (6)
Fe1-C13	1.778 (5)	O22-C22	1.131 (5)
Fe2-Fe3	2.7738 (9)	O23-C23	1.127 (5)
Fe2-H1	1.72 (5)	O31-C31	1.138 (6)
Fe2-H2	1.64 (5)	O32-C32	1.140 (5)
Fe2-C21	1.783 (5)	O33-C33	1.124 (6)
Fe2-C22	1.805 (5)	O41-C41	1.124 (6)
Fe2-C23	1.795 (4)	O42-C42	1.138 (5)
Fe3-H2	1.68 (5)	O43-C43	1.156 (5)
Fe3-C31	1.785 (5)	O44-C44	1.156 (5)
Fe3-C32	1.751 (5)		
(b) Bond Angles (deg)			
Fe1-Sb1-Fe2	68.20 (2)	C23-Fe2-Fe1	94.7 (1)
Fe1-Sb1-Fe3	67.39 (2)	C23-Fe2-Fe3	147.6 (1)
Fe1-Sb1-Fe4	141.98 (2)	Sb1-Fe2-Fe1	55.04 (2)
Fe2-Sb1-Fe3	67.71 (2)	Sb1-Fe2-Fe3	55.48 (2)
Fe2-Sb1-Fe4	137.58 (2)	Fe1-Fe2-Fe3	58.92 (2)
Fe3-Sb1-Fe4	140.14 (2)	H2-Fe3-Sb1	89 (2)
H1-Fe1-Sb1	91 (2)	H2-Fe3-Fe1	73 (2)
H1-Fe1-Fe2	34 (2)	H2-Fe3-Fe2	33 (2)
H1-Fe1-Fe3	78 (2)	H2-Fe3-C31	75 (2)
H1-Fe1-C11	77 (2)	H2-Fe3-C32	162 (2)
H1-Fe1-C12	172 (2)	H2-Fe3-C33	102 (2)
H1-Fe1-C13	93 (2)	C31-Fe3-Sb1	151.8 (2)
C11-Fe1-Sb1	150.5 (2)	C31-Fe3-Fe1	96.5 (2)
C11-Fe1-Fe2	106.7 (2)	C31-Fe3-Fe2	106.3 (1)
C11-Fe1-Fe3	94.5 (2)	C31-Fe3-C32	96.4 (2)
C11-Fe1-C12	98.2 (3)	C31-Fe3-C33	103.7 (2)
C11-Fe1-C13	103.5 (2)	C32-Fe3-Sb1	92.1 (1)
C12-Fe1-Sb1	91.2 (2)	C32-Fe3-Fe1	93.2 (2)
C12-Fe1-Fe2	147.0 (2)	C32-Fe3-Fe2	146.6 (1)
C12-Fe1-Fe3	97.0 (2)	C32-Fe3-C33	95.2 (2)
C12-Fe1-C13	93.3 (2)	C33-Fe3-Sb1	102.3 (2)
C13-Fe1-Sb1	103.8 (2)	C33-Fe3-Fe1	157.1 (2)
C13-Fe1-Fe2	101.4 (2)	C33-Fe3-Fe2	102.6 (1)
C13-Fe1-Fe3	157.8 (2)	Sb1-Fe3-Fe1	56.10 (2)
Sb1-Fe1-Fe2	56.76 (2)	Sb1-Fe3-Fe2	56.81 (2)
Sb1-Fe1-Fe3	56.51 (2)	Fe1-Fe3-Fe2	60.74 (2)
Fe2-Fe1-Fe3	60.34 (2)	C41-Fe4-Sb1	178.9 (2)
H1-Fe2-H2	70 (2)	C41-Fe4-C42	92.5 (2)
H1-Fe2-Sb1	87 (2)	C41-Fe4-C43	93.8 (2)
H1-Fe2-Fe1	31 (2)	C41-Fe4-C44	92.3 (2)
H1-Fe2-Fe3	75 (2)	C42-Fe4-Sb1	87.7 (1)
H1-Fe2-C21	173 (2)	C42-Fe4-C43	118.7 (2)
H1-Fe2-C22	83 (2)	C42-Fe4-C44	119.1 (2)
H1-Fe2-C23	92 (2)	C43-Fe4-Sb1	87.0 (1)
H2-Fe2-Sb1	89 (2)	C43-Fe4-C44	121.2 (2)
H2-Fe2-Fe1	72 (2)	C44-Fe4-Sb1	86.7 (1)
H2-Fe2-Fe3	34 (2)	Fe1-C11-O11	179.6 (6)
H2-Fe2-C21	104 (2)	Fe1-C12-O12	178.4 (5)
H2-Fe2-C22	75 (2)	Fe1-C13-O13	178.2 (5)
H2-Fe2-C23	160 (2)	Fe2-C21-O21	178.8 (4)
C21-Fe2-Sb1	90.2 (1)	Fe2-C22-O22	177.1 (5)
C21-Fe2-Fe1	144.6 (1)	Fe2-C23-O23	177.5 (5)
C21-Fe2-Fe3	97.8 (1)	Fe3-C31-O31	176.0 (5)
C21-Fe2-C22	98.5 (2)	Fe3-C32-O32	177.3 (4)
C21-Fe2-C23	94.9 (2)	Fe3-C33-O33	177.3 (5)
C22-Fe2-Sb1	163.2 (2)	Fe4-C41-O41	178.4 (5)
C22-Fe2-Fe1	113.6 (2)	Fe4-C42-O42	178.6 (5)
C22-Fe2-Fe3	108.7 (1)	Fe4-C43-O43	178.2 (4)
C22-Fe2-C23	98.6 (2)	Fe4-C44-O44	177.7 (4)
C23-Fe2-Sb1	95.0 (1)		

2.523 (12) Å in [Et₄N]₂[Sb₂Fe₃(CO)₁₇].²⁶ The Sb-Fe distance in the binary-phase of SbFe₂ is 2.59 Å.³⁰ The reason for such a long Sb-Fe bond distance in part may be the steric demands

of the four bulky Fe(CO)₄ groups. Long E-M bond distances are also observed in the analogous Bi compound [Et₄N]₃-[BiFe₄(CO)₁₆].²¹ Although these two compounds are isomorphous, the crystal quality of the antimony compound is somewhat better. It is noteworthy to compare the visible spectra of [Et₄N]₃[I] and its isoelectronic, isostructural Bi analogue. The antimony-containing compound is deep red, absorbing light at 480 nm, while the Bi-containing molecule is dark green with a band at 617 nm. The higher energy absorption for Sb is consistent with its higher first ionization potential and with the assignment of this band to a ligand-to-metal charge-transfer transition.

In compound [Et₄N]₂[II], the average Sb-Fe bond distance within the SbFe₃ tetrahedron is 2.467 (7) Å, while the Sb-Fe distance to the external Fe(CO)₄ group is longer [2.521 (2) Å]. Such a difference, however, is not so obvious in [Et₄N]₂-[Sb₂Fe₃(CO)₁₇] [2.522 (11) vs 2.529 (16) Å] and in [Et₄N]-[SbFe₄(CO)₁₄] [2.498 (33) vs 2.481 (3) Å].²⁶ Compared with the Sb-Fe bond distance in [Et₄N]₃[I], all of these bonds are much shorter. The Fe-Fe bond distances in [II]²⁻ are normal. The slightly longer Fe1-Fe3 bond distance suggests that a bridging H ligand may lie between them. The Fe-CO bond parameters support this idea, with the CO's being displaced away from the proposed μ-H location and the H ligand tilting away from the Sb atom as seen for other similar molecules. The anion is isoelectronic with a number of "spiked-tetrahedral" main-group-atom-containing clusters.³¹ In particular, it is almost identical with [Et₄N][SbFe₄(CO)₁₄],²⁶ where the μ-H ligand has been replaced by μ-CO. The doubly bridging nature of the H ligand is supported by its chemical shift (δ = -19.74 ppm), which is in the range found for related molecules: H₃BiFe₃(CO)₉ (δ = -24.1 ppm),³² H₃-BiOs₃(CO)₉ (δ = -19.9 ppm),¹⁷ H₃BiRu₃(CO)₉ (δ = -17.73 ppm),¹⁷ and [PPN][HFe₃(CO)₁₁] (δ = -14.53 ppm).³³

The structure of [Et₄N][III] is almost identical with that of [Et₄N]₂[II] except there is one more bridging H ligand. The average Sb-Fe distance within the SbFe₃ tetrahedral core is 2.479 (26) Å, while the Sb-Fe distance to the external Fe(CO)₄ group is 2.5073 (8) Å. A close look at the Sb-Fe bond distances within the core shows the distance Sb1-Fe2 [2.5088 (9) Å] is longer than the other two bond distances. This may be caused by the two H ligands, both being bound to Fe2. The two H ligands are chemically equivalent, and only one signal is observed in the ¹H NMR spectrum. Again, the doubly bridging nature of the two H ligands is supported by the chemical shift (δ = -22.63 ppm).

The crystal structure of [Et₄N]₂[IV] is virtually identical with that of [Et₄N]₃[I] except that one Fe(CO)₄ unit is replaced by Cl⁻. The average Sb-Fe bond distance in the anion is 2.565 (4) Å, much shorter than 2.666 (3) Å in [Et₄N]₃[I], and probably reflects the more favorable steric situation with the presence of the smaller Cl⁻. The Sb-Cl distance is 2.480 (2) Å, much longer than the 2.38 Å observed for SbCl₃³⁴ but comparable to the axial Sb-Cl distances of 2.52 Å in SbCl₃NH₂Ph and SbCl₃(NH₂Ph)₂.³⁴

Syntheses and Reactivities of [Et₄N]₃[I], [Et₄N]₂[II], [Et₄N][III], and [Et₄N]₂[IV]. [Et₄N]₃[I] is very reactive and an excellent precursor for the preparations of other Sb-containing compounds. It quickly reacts with trifluoromethanesulfonic acid or main-group

- (31) (a) Vites, J. C.; Eigenbrot, C.; Fehlner, T. P. *J. Am. Chem. Soc.* **1984**, *106*, 4633. (b) Shore, S. G.; Jan, D.-Y.; Hsu, L.-Y.; Hsu, W.-L. *J. Am. Chem. Soc.* **1983**, *105*, 5923. (c) Haupt, H.-J.; Neumann, F.; Preut, H. *J. Organomet. Chem.* **1975**, *99*, 439. (d) Schmid, G.; Bätzel, V.; Etzrodt, G. *J. Organomet. Chem.* **1976**, *112*, 345. (e) Gusbeth, P.; Vahrenkamp, H. *Chem. Ber.* **1985**, *118*, 1770. (f) Gusbeth, P.; Vahrenkamp, H. *Chem. Ber.* **1985**, *118*, 1746. (g) Whitmire, K. H.; Lagrone, C. B.; Churchill, M. R.; Fetting, J. C. *Inorg. Chem.* **1987**, *26*, 3491. (h) Gourdon, A.; Jeannin, Y. *J. Organomet. Chem.* **1986**, *304*, C1. (i) Lang, H.; Huttner, G.; Sigwarth, B.; Jibril, I.; Zsolani, L.; Orama, O. *J. Organomet. Chem.* **1986**, *304*, 137. (j) Hoefler, M.; Tebbe, K.-F.; Veit, H.; Weiler, N. E. *J. Am. Chem. Soc.* **1983**, *105*, 6338. (k) Richter, F.; Vahrenkamp, H. *Angew. Chem., Int. Ed. Engl.* **1978**, *17*, 444.
- (32) Whitmire, K. H.; Lagrone, C. B.; Rheingold, A. L. *Inorg. Chem.* **1986**, *25*, 2474.
- (33) Hodali, H. A.; Shriver, D. F. *Inorg. Chem.* **1979**, *18*, 1236.
- (34) Hulme, R.; Mullen, D.; Scrutton, J. C. *Acta Crystallogr., Sect. A* **1969**, *25*, S171.

(30) Holseth, H.; Kjekshus, A. *Acta Chem. Scand.* **1969**, *23*, 3043.

Table IX. Selected Bond Distances and Angles of $[\text{Et}_4\text{N}]_2[\text{IV}]$

(a) Bond Distances (Å)			
Sb1-Fe1	2.564 (1)	Fe3-C33	1.778 (8)
Sb1-Fe2	2.570 (2)	Fe3-C34	1.777 (7)
Sb1-Fe3	2.563 (1)	C11-O11	1.182 (9)
Sb1-C11	2.480 (2)	C12-O12	1.157 (9)
Fe1-C11	1.730 (8)	C13-O13	1.15 (1)
Fe1-C12	1.777 (8)	C14-O14	1.155 (9)
Fe1-C13	1.777 (9)	C21-O21	1.171 (9)
Fe1-C14	1.788 (8)	C22-O22	1.153 (8)
Fe2-C21	1.758 (8)	C23-O23	1.156 (9)
Fe2-C22	1.781 (7)	C24-O24	1.17 (1)
Fe2-C23	1.776 (8)	C31-O31	1.172 (9)
Fe2-C24	1.785 (9)	C32-O32	1.184 (9)
Fe3-C31	1.746 (8)	C33-O33	1.172 (9)
Fe3-C32	1.772 (8)	C34-O34	1.167 (8)
(b) Bond Angles (deg)			
C11-Sb1-Fe1	101.67 (5)	C23-Fe2-C24	128.0 (4)
C11-Sb1-Fe2	102.03 (6)	C24-Fe2-Sb1	85.1 (3)
C11-Sb1-Fe3	104.26 (6)	C31-Fe3-Sb1	175.6 (3)
Fe1-Sb1-Fe2	117.69 (4)	C31-Fe3-C32	91.9 (3)
Fe1-Sb1-Fe3	114.07 (4)	C31-Fe3-C33	93.4 (4)
Fe2-Sb1-Fe3	114.30 (4)	C31-Fe3-C34	92.5 (3)
C11-Fe1-Sb1	178.3 (3)	C32-Fe3-Sb1	84.2 (2)
C11-Fe1-C12	94.8 (4)	C32-Fe3-C33	121.0 (4)
C11-Fe1-C13	92.7 (4)	C32-Fe3-C34	117.4 (4)
C11-Fe1-C14	92.6 (4)	C33-Fe3-Sb1	86.9 (2)
C12-Fe1-Sb1	86.2 (3)	C33-Fe3-C34	121.0 (4)
C12-Fe1-C13	115.5 (4)	C34-Fe3-Sb1	91.0 (2)
C12-Fe1-C14	120.8 (4)	Fe1-C11-O11	179.1 (8)
C13-Fe1-Sb1	88.1 (2)	Fe1-C12-O12	177.0 (7)
C13-Fe1-C14	122.7 (3)	Fe1-C13-O13	176.5 (7)
C14-Fe1-Sb1	85.8 (2)	Fe1-C14-O14	178.3 (6)
C21-Fe2-Sb1	171.2 (2)	Fe2-C21-O21	176.9 (7)
C21-Fe2-C22	98.2 (4)	Fe2-C22-O22	176.0 (7)
C21-Fe2-C23	87.0 (3)	Fe2-C23-O23	176.0 (6)
C21-Fe2-C24	94.0 (4)	Fe2-C24-O24	176.1 (8)
C22-Fe2-Sb1	89.7 (2)	Fe3-C31-O31	178.7 (8)
C22-Fe2-C23	118.9 (4)	Fe3-C32-O32	177.3 (6)
C22-Fe2-C24	112.3 (4)	Fe3-C33-O33	177.6 (7)
C23-Fe2-Sb1	87.1 (2)	Fe3-C34-O34	175.3 (7)

halides (see Scheme I). The long Sb-Fe bond distances indicate some steric crowding about antimony, which may partially account for the degree of reactivity. The high negative charge is probably also responsible in part for the high reactivity especially toward oxidation-related reactions. It should be noted that the analogous $[\text{Et}_4\text{N}]_3[\text{BiFe}_4(\text{CO})_{16}]$ is a reactive compound and excellent precursor for the preparations of other Bi-containing compounds.²⁴

$[\text{Et}_4\text{N}]_2[\text{II}]$ is a product of the protonation-induced metal-metal bond-forming process. Previous research in our laboratory has shown that the addition of excess acid to $[\text{Et}_4\text{N}]_3[\text{BiFe}_4(\text{CO})_{16}]$ resulted in the formation of $\text{Bi}_2\text{Fe}_3(\text{CO})_9$ and $\text{H}_3\text{BiFe}_3(\text{CO})_9$, which represent products of oxidation and protonation processes, respectively;²² however, stepwise protonation was not observed. For Sb, successive addition of H^+ is seen. When the second equivalent of trifluoromethanesulfonic acid is added to $[\text{Et}_4\text{N}]_2[\text{II}]$, $[\text{Et}_4\text{N}][\text{III}]$ is formed in which another hydride ligand is added to the metal-cluster core. The addition of 2 equiv of trifluoromethanesulfonic acid to $[\text{Et}_4\text{N}]_2[\text{II}]$ results in the formation of a neutral compound that has the same IR spectrum as that of $\text{H}_3\text{BiFe}_3(\text{CO})_9$. Repeated efforts of trying to crystallize it, however, have thus far failed. The direct addition of 3 equiv of trifluoromethanesulfonic acid to $[\text{Et}_4\text{N}][\text{III}]$ leads to the formation of other uncharacterized compounds but not $\text{H}_3\text{SbFe}_3(\text{CO})_9$. This stepwise addition of acid to the antimony clusters probably reflects the way in which $\text{H}_3\text{BiFe}_3(\text{CO})_9$ is produced. The major outcome in that process, however, is not protonation but rather oxidation to give $\text{Bi}_2\text{Fe}_3(\text{CO})_9$. Oxidation also completes in the antimony system, but the product of that process is $[\text{Et}_4\text{N}]_2[\text{Sb}_2\text{Fe}_5(\text{CO})_{17}]$.

The formation of $[\text{Et}_4\text{N}]_2[\text{IV}]$ is intriguing. The product easily crystallizes in regular rectangular prisms and cubes with CH_2Cl_2

solvent. The actual chemical process by which this reaction occurs is still uncertain. Since $[\text{Et}_4\text{N}]_3[\text{I}]$ is a very good reducing agent, it is plausible that the $\text{TiCl}_3/\text{SbCl}_3$ reactions proceed via an initial redox reaction followed by substitution of $\text{Fe}(\text{CO})_4$ by Cl^- . This could explain the existence of $[\text{Et}_4\text{N}]_2[\text{IV}]$ as a byproduct in the synthesis of $[\text{Et}_4\text{N}]_3[\text{I}]$; however, more needs to be done to clarify the mechanism of this synthesis.

Comparison with Bi. Synthetically, NaSbO_3 is not a good source of Sb for these Sb-containing compounds. With $E_{\text{V/III}}^\circ$ values of 0.581 V in acid solution and -0.40 V in basic solution,³⁵ it is not as powerful an oxidant as NaBiO_3 . Sodium bismuthate, with E° of 2.03 V in its solid powder form, is an extremely powerful oxidant³⁶ and a very good source of Bi. It reacts quickly with $\text{Fe}(\text{CO})_5$ or $\text{Fe}(\text{CO})_5/\text{KOH}/\text{MeOH}$ producing $[\text{Et}_4\text{N}][\text{BiFe}_3(\text{CO})_{10}]^{19}$ and $[\text{Et}_4\text{N}]_3[\text{BiFe}_4(\text{CO})_{16}]^{21}$ in high yield, probably via the oxidation of metal-bound CO. NaSbO_3 , on the other hand, reacts only slowly with $\text{Fe}(\text{CO})_5$ under reflux, giving $[\text{Et}_4\text{N}]_2[\text{Sb}_2\text{Fe}_5(\text{CO})_{17}]$ in low yield.²⁶ With $\text{Fe}(\text{CO})_5/\text{KOH}/\text{MeOH}$, no reaction occurs. Antimony halides, however, are good starting materials. One notable difference between Bi and Sb compounds is the apparent increased tendency of the Sb atom to donate its lone pair of electrons to external metal fragments. This is rare for Bi, which prefers to be three-coordinate. Naked lone pairs are found in $\text{H}_3\text{BiFe}_3(\text{CO})_9$,³² $\text{Bi}_2\text{Fe}_3(\text{CO})_9$,¹⁷ $\text{BiCo}_3(\text{CO})_{12}$,¹³ $\text{BiMn}_3(\text{CO})_{15}$,¹⁴ $\text{BiCo}_3(\text{CO})_9$,¹⁶ $\text{Bi}_2\text{Ru}_3(\text{CO})_9$,¹⁸ $\text{Bi}_2\text{Os}_3(\text{CO})_9$,¹⁸ $\text{Bi}_2\text{Ru}_4(\text{CO})_{12}$,¹⁸ $\text{Bi}_2\text{Os}_4(\text{CO})_{12}$,¹⁸ and $[\text{Et}_4\text{N}][\text{BiFe}_3(\text{CO})_{10}]$.¹⁹ The only exceptions to this are charged clusters where the charge may promote the activity of the lone pair. On the other hand, all of the Sb-containing clusters structurally characterized to date have four-coordinate antimony atoms: $[\text{Et}_4\text{N}][\text{SbFe}_4(\text{CO})_{14}]$,²⁶ $[\text{Et}_4\text{N}]_2[\text{Sb}_2\text{Fe}_5(\text{CO})_{17}]$,²⁶ $[\text{Et}_4\text{N}]_3[\text{SbFe}_4(\text{CO})_{16}]$, $[\text{Et}_4\text{N}]_2[\text{HSbFe}_4(\text{CO})_{13}]$, $[\text{Et}_4\text{N}][\text{H}_2\text{SbFe}_4(\text{CO})_{13}]$, and $[\text{Et}_4\text{N}]_2[\text{ClSbFe}_3(\text{CO})_{12}]$.

Conclusions. Metal clusters containing antimony and iron are readily synthesized from antimony halides and iron carbonyl anions. All antimony-containing clusters characterized to date have four-coordinate Sb, while the overwhelming preference in the Bi-Fe system is toward three-coordinate Bi, suggesting a more active role for the lone pair on antimony atoms. While much of the chemistry of the Bi-Fe carbonyl system is governed by oxidation/reduction processes, the Sb-Fe system may be less active in this regard, as indicated by the favorable competition of simple protonation upon addition of acid to $[\text{Et}_4\text{N}]_3[\text{I}]$ and the observation of the subsequently protonated derivatives.

Acknowledgment. The National Science Foundation and the Robert A. Welch Foundation are gratefully acknowledged for financial support of this work. The diffractometer with which the structures reported herein were determined was obtained by the assistance of the National Science Foundation. Ivan Bernal (University of Houston) and Joseph Ferrara (Molecular Structure Corp.) are thanked for helpful discussions concerning the crystallographic determinations.

Registry No. $[\text{Et}_4\text{N}]_3[\text{I}]$, 119566-94-8; $[\text{Et}_4\text{N}]_2[\text{II}]$, 119566-96-0; $[\text{Et}_4\text{N}][\text{III}]$, 119593-12-3; $[\text{Et}_4\text{N}]_2[\text{IV}]$, 119618-96-1; SbCl_3 , 10025-91-9; $\text{Na}_2[\text{Fe}(\text{CO})_4]$, 14878-31-0; $\text{Fe}(\text{CO})_5$, 13463-40-6; SbCl_5 , 7647-18-9; Sb , 7440-36-0; Fe , 7439-89-6; $[\text{Et}_4\text{N}]_2[\text{Sb}_2\text{Fe}_5(\text{CO})_{17}]$, 118541-55-2.

Supplementary Material Available: Complete listings of X-ray diffraction parameters, anisotropic thermal parameters, U_{ij} for all atoms, atomic positional parameters for $[\text{Et}_4\text{N}]^+$ cations and bond distances and bond angles for $[\text{Et}_4\text{N}]^+$ cations (27 pages); tables of observed and calculated structure factors (150 pages). Ordering information is given on any current masthead page.

(35) Douglas, B. E.; McDaniel, D. H.; Alexander, J. J. *Concepts and Models of Inorganic Chemistry*, 2nd ed.; Wiley: New York, 1983; p 772.

(36) Cotton, F. A.; Wilkinson, G. *Advanced Inorganic Chemistry*, 5th ed.; Wiley: New York, 1988; p 430.